Response to referees

cp-2015-158

Title: ”The impact of the North American topography on the evolution of the Eurasian ice sheet over the last glacial cycle”.

By Johan Liakka, Marcus Löfverström and Florence Colleoni

———————————————

03/03/2016

We thank the referees for their insightful comments on the manuscript.

Based on the referees' comments we have done the following major structural changes to the manuscript:

- We have simplified and clarified many aspects in section 2.1 (Atmospheric simulations). First, we have removed the introduction of the "PDoro" simulations because they are not being used. Second, we have added a new subsection (2.1.1 Slab ocean model and ocean heat transport representations), where we discuss many of the aspects of our ocean representation pointed out by referee 1.

- Going hand in hand with the point above, we have re-compiled and moved the figure of the North Atlantic sea surface temperatures from the Supplement (previous Fig. S1) to the main manuscript (new Fig. 2). This figure is discussed in Section 2.1.1.

- We have modified and shortened the discussion. We have added a paragraph where we discuss our results in relation to previous studies; however, we have also moved most of the stationary wave theory to the Appendix and shortened section 4.3 (about the MIS5b ice sheet).

- We have changed the title slightly. Now it reads: "The impact of the North American glacial topography on the evolution of the Eurasian ice sheet over the last glacial cycle".

All modifications of manuscript since the last version are displayed in the ”track changes” version of our Latex code following the point-by-point reply in this document.

Best regards,
Johan Liakka, Marcus Löfverström and Florence Colleoni.

———————————————

Response to referee 1

General remarks

The objective of the authors is to model the impact of the Laurentide ice sheet on the evolution of the Eurasian ice sheet during several stages of the last glacial. Ideally, one would employ a fully coupled atmosphere-ocean-ice sheet model and make simulations over the full last glacial cycle to account for the memory of the climate system and to incorporate all feedbacks between the atmosphere, ocean and ice sheets. However, the existing comprehensive models are still rather expensive to use, implying that it is not yet feasible to perform such long experiments. One solution is to apply intermediate complexity models (e.g. Ganopolski et al. 2010). Liakka and colleagues have used an alternative approach, by running a chain of models sequentially, and by using the results of the previous step as input. The first step in this chain is the LGM simulation performed with the CCSM3 AOGCM by Brandefelt & Otto-Bliesner (2009). Secondly, these CCSM3 simulations were utilized to derive ocean heat transport (OHT) representations for the LGM and the preindustrial era that were used as a boundary condition in experiments performed with the CAM3 atmospheric GCM coupled to a mixed layer ocean model. In addition, different ice sheet configurations for MIS5b, MIS4, and LGM, based on reconstructions by Kleman et al. (2013), were also employed as boundary conditions in these CAM3 experiments. Finally, the atmospheric fields from the CAM3 experiments were applied as forcings for MIS5b, MIS4 and LGM simulations performed with the SICOPOLIS ice sheet model. The analyses presented in the paper are mostly based on the CAM3 experiments with preindustrial OHT, because the authors argue that the CAM3 experiments with LGM OHT produced a too cold climate in the North Atlantic area when compared to proxy-based temperature reconstructions.

The main result of the presented model experiments is that the Eurasian ice sheet migrates westward in MIS4 and LGM due to the impact of the growing Laurentide ice sheet on the atmospheric circulation. This result appears to be robust under different experimental setups (preindustrial and LGM OHT). The westward migration of the Eurasian ice sheet in MIS4 and LGM is consistent with reconstructions. However, in the MIS5b experiments, no westward migration of the Eurasian ice sheet is simulated, in conflict with reconstructions. The authors explain this mismatch by suggesting that under MIS5b boundary conditions, the ice sheet is not in equilibrium with the climate.

This paper deals with an important topic and the results presented are in principle of interest to the readers of Climate of the Past. However, as detailed below, I am not convinced that the experimental setup is fully appropriate to make this analysis. In my view, the main problem is that essentially all feedbacks between the ocean circulation and the ice sheet evolution are very poorly represented.

Authors' response

As we wrote in the reply during the open discussion, we do not agree that our modeling approach implies that "all feedbacks between the ocean circulation and ice sheet evolution are very poorly represented" as suggested by the referee. A slab ocean model omits the dynamic feedback but still retains the thermodynamic feedback between the ocean and the atmosphere (and thus the ice sheet evolution). Hence, any change in the atmospheric temperature would also induce changes in the SST, which in turn feed back onto the atmosphere. We have added a sentence to the methodology section (to the first paragraph of Section 2.1.1.) where we emphasize this.

Main comments

- The presented analysis for MIS5b, MIS4 and LGM is mainly based on experiments with a preindustrial OHT. The authors argue that the LGM OHT was inducing too cold conditions in the Atlantic Ocean, with a too extensive sea ice cover. Ideally, one would use specific OHT

representations from experiments specifically designed for MIS5b, MIS4 and LGM. In my view, using the preindustrial OHT is really problematic, and is very likely to produce results that are not meaningful for the last glacial conditions, as it is very clear from palaeoceanographic evidence that the LGM North Atlantic Ocean was substantially colder than during the preindustrial era. I would argue that it makes much more sense to use the LGM OHT. There is evidence that in the North Atlantic Ocean the sea ice cover was extending to at least 45N (e.g., Renssen & Vandenberghe, 2003). This would suggest that, at least for the LGM time slice, the results obtained with LGM OHT are more appropriate. I assume that the applied LGM OHT is based on the LGM2 state of Brandefelt & Otto-Bliesner (2009). I would argue that their LGM1 state would have been even more appropriate, as this state represents a stronger AMOC and less cold North Atlantic Ocean compared to the LGM2 state. In Otto-Bliesner et al. (2006), the simulated SSTs of LGM1 are compared to reconstructions, showing a good fit. I therefore strongly suggest repeating the analysis with CAM3 and SICOPOLIS with an OHT based on the LGM1 state.

Authors' response

As we discussed more comprehensively in the previous reply, preindustrial (PI) OHT does not yield PI SST. The OHT is included as a prescribed monthly climatology in the slab ocean model, but the SSTs are ultimately determined by the surface energy balance (see e.g. Collins et al. 2004; Bitz et al. 2012). As a consequence, the North Atlantic SSTs are substantially colder and the sea-ice cover is increased at LGM (relative to present-day) also when using PI OHT; in fact, the sea-ice margin extends even further south than 45N in western North Atlantic in the LGM simulation with PI OHT (see the new Fig. 2 in the manuscript).

All this information was previously compiled in Fig. 1 in the Supplement (we admit that the figure was not very easy to interpret), but because of its relevance for motivating our experiments we have chosen to re-work the figure and move it to the main manuscript (new Fig. 2). The figure shows the annual mean North Atlantic (LGM-PI) SST anomalies in the simulations with (a) PI OHT and (b) LGM OHT as well as (c) the fully-coupled LGM simulation in CCSM4 (data from Brady et al. 2013). It also shows the equivalent SST anomalies from the MARGO proxy data (Margo project members, 2009). We discuss this figure in detail in Section 2.1.1; however, in summary it illustrates that both the North Atlantic SSTs and sea-ice cover in the proxy reconstructions are in better agreement with the LGM simulation with PI OHT than the simulation with LGM OHT. For example, similar to several post-CLIMAP reconstructions (Paul and Schaefer 2003; Toracinta et al. 2004; de Vernal et al. 2005, 2006; Margo project members 2009) the sea-ice cover is reduced in the eastern North Atlantic in the PI OHT simulation, whereas the LGM simulation yields a zonal CLIMAP-like equatorward sea-ice margin. Thus, contrary to the referee, we believe it is meaningful to use PI OHT in our study, not the least because it yields a better agreement with the North Atlantic SST proxy than when using LGM OHT.

The reason why LGM OHT yields such cold SSTs and extensive sea-ice cover in the North Atlantic is due to a strong reduction of the LGM AMOC strength in CCSM3 (Brandefelt and Otto-Bliesner 2009). This response is model specific as other atmosphere-ocean models yield completely different AMOC responses for the LGM (e.g. Weber et al. 2007). For example, the more recent NCAR model, CCSM4, yields no significant weakening of the LGM AMOC (it even yields a strengthening in the lower midlatitudes; Brady et al. 2013). Brady et al. (2013) found that the LGM simulation with CCSM4 is in very good agreement with the MARGO proxy (see also Fig. 2c in the new manuscript).

We realize, however, that using the term "LGM OHT" to describe the OHT from the LGM2 state in Brandefelt and Otto-Bliesner (2009) is somewhat confusing since it may sound like we use the OHT that actually prevailed at the LGM rather than a OHT field from one specific model. To better reflect from where the OHT was derived. we have decided to change "LGM OHT" to "BO2009 OHT" throughout the entire manuscript.

There are three reasons why we do not believe it is necessary to conduct new simulations using the LGM1 OHT state from Brandefelt and Otto-Bliesner (2009):

1. The simulations with PI OHT yield sufficiently cold ocean surface temperatures at LGM, and the resulting North Atlantic sea-ice cover agrees well with the LGM reconstructions (see argument above).

2. The stationary wave response to the North American glacial topography -- upon which we base our conclusions -- is not that sensitive to the OHT representation (compare Figs. 3 and 5 in the main manuscript to Figs. 4 and 6 in the Supplement). Hence, it is very unlikely that using the "intermediate" LGM1 state would radically alter the stationary wave response and thereby yield other conclusions.

3. The LGM1 state is not completely in steady-state (Brandefelt and Otto-Bliesner 2009). This is a very important point because our objective here is to use the OHT for steady-state experiments with the slab ocean model. Although the climate in such simulation would equilibrate at some point, the resulting equilibrium state would never be in true steady-state because of the non-equilibrated OHT.

All points above are emphasized in the new manuscript (point 1 and 3 in section 2.1.1, and point 2 in the abstract).

- As noted, the LGM OHT used in the CAM3 experiments is derived from the CCSM3 simulations of the LGM climate. In my view, it is important to establish if the CCSM3 LGM climate is consistent with the LGM climate simulated by the CAM3 model. The atmospheric components in both models are basically the same (CAM3), but the two setups have different resolutions, very different ocean models and the simulations use different boundary conditions, e.g. the ice sheet configurations. If the climates are not consistent, I would argue that the CCSM3-derived LGM OHT should not be used in the CAM3 experiments.

Authors' response

It is difficult to know what the referee means by ”consistent” here. Do they have to be identical? Or just very similar? But yes, the large-scale features of our LGM simulation (with LGM ”BO2009” OHT) are very similar to the LGM2 state climate in Brandefelt and Otto-Bliesner (2009). The similarity is hinted in Fig. 2b which shows a zonal sea-ice margin in the North Atlantic at around 40N, thus essentially identical to the LGM2 state sea-ice margin in Brandefelt and Otto-Bliesner (2009). Also features such as the global annual mean temperature and the equator-to-pole temperature gradient are very similar between the simulations (for details; see Löfverström et al. 2014). However, as the referee points out, the boundary conditions used here and in Löfverström et al. (2014) are not identical to Brandefelt and Otto-Bliesner (2009). Perhaps most importantly, the simulations employed different representations of the LGM ice-sheet topography; here (and in Löfverström et al. 2014) we used the ice-sheet reconstructions from Kleman et al. (2013) whereas Brandefelt and Otto-Bliesner (2009) used the ICE-5G glacial topography (Peltier 2004). The ICE-5G LGM reconstruction has a substantially higher ice dome (~1000 m) in North America than in Kleman et al. (2013). Therefore one cannot not expect the responses to be completely identical between the simulations.

If, however, all boundary conditions were in fact the same as in Brandefelt and Otto-Bliesner (2009) the results would be practically identical. This is obvious because the OHT was derived from their simulation and because we use the same atmospheric model. Hence, both the OHT and surface energy balance would be the same in both simulations; thus, in steady-state (the sea-surface temperature tendency is zero, dT/dt=0) the SSTs would be identical (for the slab ocean model equation; see e.g. Bitz et al. 2012 or our reply in the open discussion). Note, however, that this would not necessarily be the case if we would use the LGM1 state to derive the OHT. Since the LGM1 state is not in steady-state the temperature tendency (dT/dt) is not zero; this ”error” would then be compensated by changes in the surface energy balance.

The motivation for using a slab ocean model is highlighted in the first paragraph of section 2.1.1. In addition, we have added the following footnote to section 2.1.1 that discusses the consistency with the fully-coupled simulation from Brandefelt and Otto-Bliesner (2009): *"Note that the sea-ice cover in Fig. 2b is virtually identical to the one obtained in Brandefelt and Otto-Bliesner (2009) (see their Fig. 2), indicating that our slab ocean simulation is consistent with the fully-coupled simulation from which the OHT was derived."*

- If understand correctly Löfverström et al. (2014), a modern annual-mean mixed layer depth is applied in the slab ocean model to specify the ocean's heat capacity in all the glacial experiments used in the present study. Why was this done and what is the impact on the results? I propose to explain this in the methodology section.

Authors' response

The mixed layer depth is important as it controls the response time of the ocean temperature to changes in the surface energy balance. The LGM winds are generally stronger than in the PI climate, especially in midlatitudes in the North Atlantic sector. However, it is not only the strength of the winds field that is influenced by the LGM boundary conditions, but also the orientation and spatial location of the circulation anomalies. Löfverström et al. (2014) found, in accordance with Li and Battisti (2008), that the LGM winter jet is stronger, more zonal and spatially confined compared to the PI climate. These changes in isolation yield a deeper mixed layer extending rather zonally across the North Atlantic basin. However, Brandefelt and Otto-Bliesner (2009) found that the LGM mixed layer depth in the North Atlantic actually decreases somewhat when the model equilibrates. No explanation for this result was provided, but it is likely due to the expansion of the sea-ice cover that reduces the mixing effect of the wind; figure 1 in Brandefelt and Otto-Bliesner (2009) shows a mixed layer depth in the GIN seas of about 100 m in the equilibrated LGM state, which is comparable to the PI counterpart.

We used the PI mixed layer depth because the LGM correspondence was not saved on the CCSM3 data server. It is not obvious how changes in the ocean mixed layer depth would influence our results, but according to the results presented in Brandefelt and Otto-Bliesner (2009), the largest changes in the North Atlantic region (of order 50-100 m) are found where the sea-ice cover is perennial in both the LGM simulation and in proxy data, which suggests that the PI mixed layer depth works equally well in these regions as there is virtually no heat exchange between the atmosphere and ocean. The changes elsewhere are smaller (of order 10 m; see Fig. 4e in Brandefelt and Otto-Bliesner 2009), suggesting that the effect of changes in the mixed layer depth likely is small.

We have added the following sentence to section 2.1.1 regarding this issue: *"Aside from areas covered by perennial sea ice, simulated changes of the LGM mixed-layer depth are small compared to PI (of order 10 m; Brandefelt and Otto-Bliesner 2009); following Löfverström et al. (2014) we therefore use a modern annual mean mixed-layer depth in all simulations."*

- In my view Section 4 could be improved by discussing the obtained results relative to previous studies on the evaluation of ice sheets, for instance Ganopolski et al. 2010 and Beghin et al. 2014. Are the results consistent? If not, what is the reason?

Authors' response

Good idea. The third paragraph in the modified Discussion section now contains a discussion of our results in relation to previous studies (primarily Beghin et al. 2014).

Minor comments

- Figures 2, 3, 4: I wonder what the statistical significance is of the simulated anomalies. I suggest to perform a test (e.g. t-test for temperature) and to show only results that are statistically significant.

Authors' response
We have followed the referee's suggestion and used a Students t-test (at 95% confidence level) to test the statistical significance of the simulated anomalies in panels (d), (f) and (g) of the old Figs. 2, 3, 4 (now Figs. 3, 4, 5) and Figs. 4, 5 and 6 in the Supplement. In addition we have added the following sentence to the captions of the figures above: "*The colored shading in (d,f,h) shows only statistically significant values based on a Student's t-test (at the 95% confidence level).*" Note, however, since we use fairly many years (25 years) to create the climatology nearly all the grid points that previously attained values covered by the colored shading in those figures are statistically significant according to the t-test.

- Page 5205, line 6. "The stadials are referred to as the Marine Isotope Stages (MIS) 5d (106-115 kyrs BP), 5b (85-93 kyrs BP), 4 (60-74 kyrs BP) and 2 (12-24 kyrs BP". This sentence is confusing, as the meaning of stadials is not identical to that of Marine Isotope Stages. For instance, MIS4 includes 3 stadials according to the Greenland ice core record (e.g. Rasmussen et al. 2014) and MIS3 also includes stadials. So I suggest rephrasing.

Authors' response

Thanks for pointing it out. We have rephrased the introduction.

- Section 2.1: I suggest including more information on the experimental setup, particularly the CAM3 experiments. For instance, for how many years have the CAM3 experiments been run? I suggest including a table with all boundary conditions and forcings. A flow diagram that explains the full experimental setup would also help.

Authors' response

We agree that section 2.1 was previously a little bit confusing, especially because we introduced the ”PDoro” simulations but never really discussed them in the subsequent parts of manuscript. We hope that the new version of section 2.1 is a little bit less confusing and easier to follow. We have added a sentence about that we average over 25 years to create the climatologies for analysis in CAM3. In the new 2.1 section we do not believe it is necessary to include flow diagram or an additional table to Table 1, which already shows the orbital fording and greenhouse gas concentrations used for all glacial time slices. For each glacial time slice we only use two different sets of topography (EAonly and fullGlacial) and OHT (PI and BO2009). We hope it is easy for the reader to understand this without a specific table in the new manuscript version.

- Page 5210, line 26: To estimate the fractions of solid and liquid precipitation, a limiting temperature is set. If the temperature is less than -10C, all precipitation is solid, and if it is above 7C, all precipitation is liquid. Between these temperatures, there are varying fractions solid and liquid precipitation. I was wondering what the rationale is for using -10C and 7C? On what are these values based?

Authors' response

See also our reply to Referee 2. The temperature limits for liquid and solid precipitation are based on Marsiat (1994). These values are default in SICOPOLIS (see e.g. Greve et al. 1999; Greve et al. 2011), but has been used also in other ice sheet models (Langen et al. 2012). We have added the Marsiat reference to the ice-sheet model section.

- Page 5212, 2nd paragraph, starting line 11: Please clarify what experiments you compare here. Only the EA-only simulations, or also the fullGlacial runs?

Authors' response

Thanks for pointing it out. It refers to the EAonly simulation. We have clarified this in the text.

- Figure 6: Is the longitude for the Eurasian ice sheet mass centre for the EAonly experiment on MIS4 consistent with Figure 5c? Visual inspection of the latter figure suggests that the centre of mass in the Barents Sea at ~30E, while Figure 6 suggests ~55E. How is the centre of mass defined?

Authors' response

Yes, it is consistent. The longitude of the center of mass (λ_c) is defined over the entire Eurasian continent. This implies that the relatively small ice sheet in eastern Siberia in the EAonly simulation also contributes by increasing λ_c. Hence, λ_c should be interpreted as the "average longitude of ice in Eurasia" rather than the "average longitude of the largest ice sheet in Eurasia". We have clarified this in the text and the figure caption.

- Page 5222, line 8: "between the MIS4 and LGM extents and the proxy suggests..." I propose to replace "proxy" by "proxies"

Authors' response

We have changed "proxy" to "reconstructions" which we believe is even more accurate.

- Page 5223, line 17: should be "yields cooler summer temperatures" - Page 5223, line 22: should be "an equivalent"

Authors' response

Thanks for pointing it out. We have changed this in the manuscript.

- Page 5224, line 13: should be "our results are"

Authors' response

Thanks again. We have change this too.

Response to Referee 2

Specific comments

- The main results in the paper are based on simulations using the preindustrial modeled ocean heat transport. The authors also show that the main result of the paper, namely that the Eurasian ice sheet is shifted westward by the changes in atmospheric circulation induced by the Laurentide ice sheet, strongly depend on the ocean heat transport used. The westward shift is actually much less pronounced if the modeled LGM ocean heat transport is used. The authors should make this clear in the abstract and the conclusions.

Authors' response

Thanks for the tip. We have added some sentences about this ocean heat transport aspect in the abstract and conclusions.

- The authors should discuss the assumption that climate and ice sheets are at equilibrium during the simulated time slices in some more detail. What is the possible role of the ice sheet history for the actual ice sheet state at the simulated stages?

Authors' response

This is an important topic, which has received a lot of attention in past studies (e.g. Calov and Ganopolski 2005; Abe-Ouchi et al. 2013). Unfortunately, it is difficult to investigate this topic accurately with the current model setup since we would preferably want to use transient coupled climate-ice sheet simulations; thus practically impossible using CAM3 at T85 resolution. However, based on the equilibrium simulations at hand, we have done some first-order sensitivity simulations regarding this issue. These simulations are briefly discussed in Section 4.3 (note that 4.3 deals with the lack of ice growth at MIS5b so the discussion evolves mostly around the MIS5b case, although we mention also MIS4 and LGM):

"*In addition, we fail to find multiple equilibrium states (e.g. Calov and Ganopolski 2005; Abe-Ouchi et al. 2013) of the simulated Eurasian ice sheets (Fig. 7 in the Supplement); initializing the ice-sheet simulations using the Kleman et al. (2013) reconstructions leads to very similar equilibrium extents as in Fig. 6 .This suggests that preceding configurations of the Eurasian ice sheet were not crucial for maintaining the ice sheet at MIS5b.*

Instead, it is more likely that the MIS5b ice sheet was not in equilibrium with the prevailing climate. The successful glacial inception and good agreement between the equilibrated MIS4 and LGM ice sheets and the reconstructions suggests that the climate was locally cold enough to support glacial inception and the resulting ice sheets were in equilibrium with the prevailing climate; this is, however, not necessarily true for MIS5b. Instead, it is plausible that the MIS5b climate was too warm to support glacial inception and the ice sheet was a remnant of ice growth in preceding colder periods. In this context it is interesting to note that the Eurasian ice sheet reached a size comparable to MIS5b already at ~105 kyrs BP, subsequent to a relative minimum in the high-latitude boreal summer insolation (Kleman et al. 2013; Löfverström et al. 2014)."

Fig. 7 in the Supplement shows that even if using large-scale ice sheets as a initial condition (as opposed to bare ground) the equilibrium extents converge toward more or less the same as in Fig. 6. Hence, if the climate remains constant, the ice-sheet history is not crucial for the simulated extents in our study. In addition, the good agreement between the simulated equilibrium extents of the MIS4 and LGM ice sheets in Eurasia and the proxy-based reconstructions suggests that the transient climate history was not that crucial either for obtaining the observed ice-sheet extents. At MIS5b, however, we have to impose an artificial cooling to get sufficient ice growth (Fig. 9 in the manuscript). This indicates that the MIS5b ice sheet expanded earlier during colder conditions.

- The separation of precipitation into rainfall and snowfall based on temperature between -10C and +7C seems somehow arbitrary to me. Are the model results sensitive to this particular choice?

Authors' response

See also our reply to Referee 1. Those specific numbers in the snowfall-to-rainfall-ratio parameterization are default in the model and based on Marsiat (1994). The model results are not particularly sensitive to this parameter choice. Figure 1 in the attachment to this response letter shows the simulated ice thickness at LGM (EAonly in panel a and fullGlacial in b) using, respectively, -3C and +3C as temperature limits for snow and rain as opposed to -10C and 7C in Fig. 6 in the manuscript. The resulting ice extents in Fig. 1 in this letter are very similar to those in Fig. 6e,f, suggesting that our results are not that sensitive to the specific values of the rain/snow temperature limits. As long as the average between the snowfall and rainfall temperature limit is close to 0C (which obviously makes sense) changing the limits has only a small effect on the ice sheet evolution. More specifically, changes in the precipitation/snowfall partitioning could speed up or slow down the growth of the ice sheet by modulating the accumulation; however, it would not have any significant impact of the equilibrium extent of the ice sheet, which is primarily determined by the location of the 0C isotherm of the summer temperature.

We have added the Marsiat reference to ice-sheet model section.

Technical comments

Page 5212, line 19: ERA-Intirim -> Era Interim

Authors' response

According to the main reference (Dee et al. 2011) our spelling is correct; see http://onlinelibrary.wiley.com/doi/10.1002/qj.828/full

Page 5215, line 10: "high latitude height anomalies". Please specify that it is geopotential height.

Authors' response

Thanks, we have changed this throughout the manuscript.

Page 5219, line 7: "a monotonically decreasing" should be "monotonically decreasing"

Authors' response

Thanks, we have changed this.

Page 5223, line 17: "yields a cooler summer" should be "yields cooler summer"

Authors' response

Thanks.

Page 5223, line 21: "a equivalent" -> "an equivalent"

Authors' response

Thanks.

Page 5223, line 21: here and elsewhere in the paper please specify that you are referring to cyclonic and anticyclonic ANOMALIES and not absolute values.

Authors' response

Thanks, we have changed this throughout the manuscript.

Page 5224, line 13: "our results is" -> "our results are"

Authors' response

Thanks.

References

Abe-Ouchi, A., Saito, F., Kawamura, K., Raymo, M. E., Okuno, J., Takahashi, K., and Blatter, H.: Insolation- driven 100,000-year glacial cycles and hysteresis of ice-sheet volume, Nature, 500, 190–193, 2013.

Bitz, C. M., Shell, K., Gent, P., Bailey, D., Danabasoglu, G., Armour, K., Holland, M., and Kiehl, J.: Climate sensitivity of the community climate system model, version 4, Journal of Climate, 25, 3053–3070, 2012.

Brady, E. C., Otto-Bliesner, B. L., Kay, J. E., and Rosenbloom, N.: Sensitivity to glacial forcing in the CCSM4, Journal of Climate, 26, 1901–1925, 2013.

Brandefelt, J. and Otto-Bliesner, B. L.: Equilibration and variability in a Last Glacial Maximum climate simulation with CCSM3, Geophys. Res. Lett., 36, L19712, doi:10.1029/2009GL040364, 2009.

Calov, R. and Ganopolski, A.: Multistability and hysteresis in the climate-cryosphere system under orbital forcing, Geophysical research letters, 32, 2005.

Collins, W. D., Rasch, P. J., Boville, B. A., Hack, J. J., McCaa, J. R., Williamson, D. L., Kiehl, J. T., Briegleb, B., Bitz, C., Lin, S., et al.: Description of the NCAR community atmosphere model (CAM 3.0), Tech. Note NCAR/TN-464+ STR, NCAR, 2004.

De Vernal, A., Eynaud, F., Henry, M., Hillaire-Marcel, C., Londeix, L., Mangin, S., Matthießen, J., Marret, F., Radi, T., Rochon, A., et al.: Reconstruction of sea-surface conditions at middle to high latitudes of the Northern Hemisphere during the Last Glacial Maximum (LGM) based on dinoflagellate cyst assemblages, Quaternary Science Reviews, 24, 897–924, 2005.

De Vernal, A., Rosell-Melé, A., Kucera, M., Hillaire-Marcel, C., Eynaud, F., Weinelt, M., Dokken, T., and Kageyama, M.: Comparing proxies for the reconstruction of LGM sea-surface conditions in the northern North Atlantic, Quaternary Science Reviews, 25, 2820–2834, 2006.

Dee, D. P., Uppala, S. M., Simmons, A. J., Berrisford, P., Poli, P., Kobayashi, S., Andrae, U., Balmaseda, M. A., Balsamo, G., Bauer, P., Bechtold, P., Beljaars, A. C. M., van de Berg, L., Bidlot, J., Bormann, N., Delsol, C., Dragani, R., Fuentes, M., Geer, A. J., Haimberger, L., Healy, S. B., Hersbach, H., Hólm, E. V., Isaksen, L., Kållberg, P., Köhler, M., Matricardi, M., McNally, A. P., Monge-Sanz, B. M., Morcrette, J.-J., Park, B.-K., Peubey, C., de Rosnay, P., Tavolato, C., Thépaut, J.-N., and Vitart, F.: The ERA-Interim reanalysis: configuration and performance of the data assimilation system, Quart. J. Roy. Meteor. Soc., 137, 553–597, 2011.

Greve, R., Wyrwoll, K.-H., and Eisenhauer, A.: Deglaciation of the Northern Hemisphere at the onset of the Eemian and Holocene, Annals of Glaciology, 28, 1–8, 1999.

Greve, R., Saito, F., and Abe-Ouchi, A.: Initial results of the SeaRISE numerical experiments with the models SICOPOLIS and IcIES for the Greenland ice sheet, Annals of Glaciology, 52, 23–30, 2011.

Kleman, J., Fastook, J., Ebert, K., Nilsson, J., and Caballero, R.: Pre-LGM Northern Hemisphere ice sheet topography, Climate of the Past, 9, 2365–2378, doi:10.5194/cp-9-2365-2013, 2013.

Langen, P. L., Solgaard, A. M., and Hvidberg, C. S.: Self-inhibiting growth of the Greenland Ice Sheet, Geophysical Research Letters, 39, 2012.

Li, C. and Battisti, D.: Reduced Atlantic Storminess during Last Glacial Maximum: Evidence from a Coupled Climate Model, Journal of Climate, 21, 3561–3579, 2008.

Löfverström, M., Caballero, R., Nilsson, J., and Kleman, J.: Evolution of the large-scale atmospheric circulation in response to changing ice sheets over the last glacial cycle, Climate of the Past, 10, 1453–1471, doi:10.5194/cp-10-1453-2014, 2014.

Margo Project Members, Waelbroeck, C., Paul, A., Kucera, M., Rosell-Melé, A., Weinelt, M., Schneider, R., Mix, A. C., Abelmann, A., Armand, L., Bard, E., Barker, S., Barrows, T. T., Benway, H., Cacho, I., Chen, M.-T., Cortijo, E., Crosta, X., de Vernal, A., Dokken, T., Duprat, J., Elderfield, H., Eynaud, F., Gersonde, R., Hayes, A., Henry, M., Hillaire-Marcel, C., Huang, C.-C., Jansen, E., Juggins, S., Kallel, N., Kiefer, T., Kien- ast, M., Labeyrie, L., Leclaire, H., Londeix, L., Mangin, S., Matthiessen, J., Marret, F., Meland, M., Morey, A. E., Mulitza, S., Pflaumann, U., Pisias, N. G., Radi, T., Rochon, A., Rohling, E. J., Sbaffi, L., Schäfer-Neth, C., Solignac, S., Spero, H., Tachikawa, K., and Turon, J.-L.: Constraints on the magnitude and patterns of ocean cooling at the Last Glacial Maximum, Nature Geoscience, 2, 127–132, doi:10.1038/ngeo411, 2009.

Marsiat, I.: Simulation of the Northern Hemisphere continental ice sheets over the last glacial-interglacial cycle: experiments with a latitude-longitude vertically integrated ice sheet model coupled to a zonally averaged climate model, Paleoclimates, 1, 59–98, 1994.

Paul, A. and Schäfer-Neth, C.: Modeling the water masses of the Atlantic Ocean at the Last Glacial Maximum, Paleoceanography, 18, 1058, doi:10.1029/2002PA000783, 2003.

Peltier, W.: Global glacial isostasy and the surface of the ice-age Earth: the ICE-5G (VM2) model and GRACE, Annu. Rev. Earth Planet. Sci., 32, 111–149, 2004.

Toracinta, E. R., Oglesby, R. J., and Bromwich, D. H.: Atmospheric Response to Modified CLIMAP Ocean Boundary Conditions during the Last Glacial Maximum(., Journal of Climate, 17, 504–522, 2004.

Weber, S., Drijfhout, S., Abe-Ouchi, A., Crucifix, M., Eby, M., Ganopolski, A., Murakami, S., Otto-Bliesner, B., and Peltier, W.: The modern and glacial overturning circulation in the Atlantic ocean in PMIP coupled model simulations, Climate of the Past, 3, 51–64, 2007.

Figures

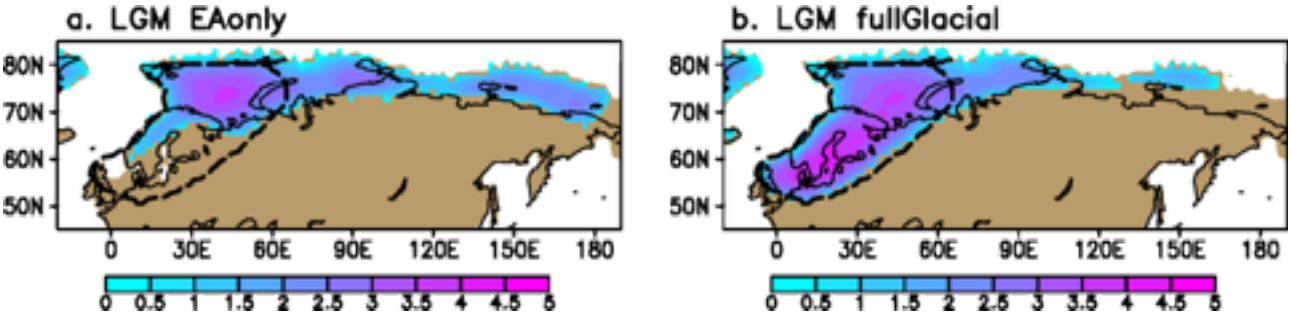

Figure 1: Same as Fig. 6e,f in the main manuscript except for using -3C and +3C, respectively, as the temperature limits for snow and rain in the Marsiat (1994) parameterization.

Manuscript track changes

\documentclass[cp, manuscript]{copernicus}

\begin{document}

\linenumbers

\title{The impact of the North American glacial topography~~ice sheet~~ on the evolution of the Eurasian ice sheet ~~during~~over the last glacial cycle}

\Author[1]{Johan}{Liakka}
\Author[2]{Marcus}{L\"{o}fverstr\"{o}m}
\Author[3]{Florence}{Colleoni}

\affil[1]{Biodiversity and Climate Research Centre, Senckenberg Gesellschaft f\"{u}r Naturforschung, Senckenberganlage 25, 60325 Frankfurt am Main, Germany.}
\affil[2]{National Center for Atmospheric Research, 1850 Table Mesa Drive, 80305 Boulder, CO, USA.}
\affil[3]{Centro Euro-Mediterraneo sui Cambiamenti Climatici, via Franceschini 31, 40128 Bologna, Italy.}

\runningtitle{North American impact on the Eurasian ice sheet}

\runningauthor{Liakka et al.}

\correspondence{Johan Liakka (johan.liakka@senckenberg.de)}

\received{}
\pubdiscuss{}
\revised{}
\accepted{}
\published{}

\firstpage{1}

\maketitle

\begin{abstract}
Modeling studies ~~show~~have shown that the ~~massive~~continental scale ice sheets in North America and Eurasia ~~expanding over the North American and Eurasian continents~~ in the last glacial cycle has ~~ds~~ a large ~~impact~~influence on the atmospheric ~~stationary waves~~ circulation and thus yielded a ~~glacial~~ climate distinctly different from the present. However, to what extent the two ice sheets influenced each others growth trajectories remains largely unexplored. In this study we investigate how an ice sheet~~s~~ in North America influence~~s~~ the downstream evolution of the Eurasian ice sheet, using a thermomechanical ice-sheet model forced by climate data from atmospheric snapshot ~~simulations~~experiments of three distinctly different phases of the last glacial cycle: the Marine Isotope Stages 5b, 4 and 2 (LGM). Owing to the large uncertainty associated with glacial changes of the Atlantic meridional overturning circulation, each atmospheric snapshot experiment was conducted using two distinctly different ocean heat transport representations. Our results suggest that changes in the North American paleo-topography may have ~~had a large influence on evolution of the Eurasian ice sheet~~ largely controlled the zonal distribution of the Eurasian ice sheet. In the MIS4 and LGM experiments, the Eurasian ice sheet migrates westward towards the Atlantic sector -- largely consistent with geological data and contemporary ice-sheet reconstructions -- due to a

low wavenumber stationary wave response, which yields a cooling in Europe and a warming in northeastern Siberia. The expansion of the North American ice sheet between MIS4 and LGM amplifies the Siberian warm anomaly, which limits the glaciation there and may therefore help ~~to~~ explain the progressive westward migration of the Eurasian ice sheet ~~over~~in this time period. The ocean heat transport has only a small influence on the stationary wave response to the North American glacial topography; however, because temperature anomalies have a smaller influence on an ice sheet's ablation in a colder climate than in a warmer one, the impact of the North American glacial topography on the Eurasian ice-sheet evolution is reduced for colder surface conditions in the North Atlantic. While the Eurasian ice sheet in the MIS4 and LGM experiments appears to be in equilibrium with the simulated climate conditions, the MIS5b climate forcing is too warm to grow an ice sheet in Eurasia. First-order sensitivity experiments suggest that most of the MIS5b ice sheet was established during preceding colder stages.
\end{abstract}

\introduction
The Quaternary period is characterized by the alternation between cold and warm phases -- glacial and interglacials -- when massive ice sheets expand and retreat over the subpolar continents. The last glacial cycle began about 115 000 years ago (115 kyrs BP) following a minimum in the boreal summer insolation \citep{berger+loutre1991}. Over the subsequent $\sim$90 kyrs, paleo-records suggest that ice sheets progressively expanded in North America and Eurasia, with ~~periods of~~ relatively rapid ice growth during colder phases ~~(stadials)~~ followed by warmer periods ~~(interstadials)~~ when the global ice volume remained relatively constant \citep{peltier +fairbanks2006,stokes_etal2012,kleman_etal2013}. The ~~stadials~~colder phases ~~are~~ typically referred to as the Marine Isotope Stages (MIS) 5d (106-115 kyrs BP), 5b (85-93 kyrs BP), 4 (60-74 kyrs BP) and 2 (12-24 kyrs BP), where the latter includes the culmination of the last glacial cycle at the Last Glacial Maximum (LGM; 19-23 kyrs BP).

The progressive increase of the Northern Hemisphere ice volume was dominated by the Laurentide and Cordilleran ice sheets in North America \citep[][]{kleman_etal2013}. Subsequent to the ice-sheet inception in the Canadian Arctic and Quebec, the Laurentide ice sheet expanded over the eastern parts of the continent and eventually coalesced with the Cordilleran ice sheet to form a coherent and continent-wide ice sheet at the LGM \citep[Fig.\ \ref{fig:kleman};][] {clark_etal1993,kleman_etal2010,kleman_etal2013}. As opposed to the North American counterpart, the combined volume of the Eurasian ice sheets (Fennoscandian and Barents-Kara ice sheets) changed relatively little between the inception phase and LGM \citep[Fig.\ \ref{fig:kleman};][]{svendsen_etal2004,kleman_etal2013}. Instead, the most notable feature of the ice-sheet evolution in Eurasia is a progressive westward migration in time; in the early and intermediate stages (MIS5b and MIS4) the eastern margin of the Eurasian ice sheet was located in central Siberia \citep[][]{svendsen_etal2004,kleman_etal2013}, whereas essentially only northern Europe and the British Isles \citep[][]{bradwell_etal2008} were ice covered at the LGM (Fig.\ \ref{fig:kleman}). Hence, in both ~~the~~ North America~~n~~ and Eurasia~~n continents~~, the ice sheets had strong zonal asymmetries toward the Atlantic sector over large parts of the glacial cycle. The driving mechanism of this asymmetry remains an open question as it has been difficult to capture this feature in conventional ice-sheet model experiments \citep{marshall_etal2000,zweck +huybrechts2005,charbit_etal2007,bonelli_etal2009,beghin_etal2014}.

The role of ice sheet-atmosphere interactions has mostly been studied for the build-up of the North American ice sheet \citep{roe +lindzen2001,liakka_etal2011,lofverstrom_etal2014,lofverstrom_etal2015}~~s in North America~~. These studies suggest that the east-heavy pre-LGM configuration arose from changes in the time-mean atmospheric circulation (stationary waves) forced by the ice sheet itself, possibly in combination with complex interactions with the North American Cordillera ~~\citep{roe +lindzen2001,liakka_etal2011,lofverstrom_etal2014,lofverstrom_etal2015}~~. The ~~mechanisms behind the~~ temporal evolution of the Eurasian ice sheet ~~have~~has received less attention. The orographic precipitation feedback, initially proposed by \cite{sanberg+oerlemans1983}, is generally considered an important feature to explain the westward migration of the ice sheet \citep{roe

+lindzen2001,van_etal2008,liakka+nilsson2010,kleman_etal2013,lofverstrom_etal2014} as. Ssurface winds from the Atlantic are forced vertically by the western and southern slopes of the ice sheet, hence leading to increased precipitation rates in those regionsareas and ultimately to a (south)westward propagation of the ice sheet \citep{sanberg+oerlemans1983}. Although orographic precipitation is a robust feature in moist atmospheric general circulation models \citep{roe2005}, questions regarding the timing of the westward migration of the Eurasian ice sheet remain unanswered. For example, why did the Eurasian ice sheet propagate westward only in the latter stages of the glacial cycle and not immediately subsequent to the inception phase? The answer to this question is complicated by the fact that the orientation of the Atlantic storm track, which has a large impact on the European precipitation, appears to be controlled by the size of the North American ice sheet; for smaller ice sheets in North America (e.g.\ MIS5b and MIS4) the Atlantic storm track has a pronounced southwest-northeast tilt \citep[{similar to the modern climate][]{lofverstrom_etal2014,pausata+lofverstrom2015}}, whereas for large ice sheets (LGM) the storm track has a more zonal orientation \citep{li+battisti2008,kageyama_etal2013,lofverstrom_etal2014,ullman_etal2014,merz_etal2015,pausata+lofverstrom2015}. The zonalisation of the Atlantic storm track typically yields drier (wetter) conditions in northern (southern) Europe \citep{lofverstrom_etal2014}.

The connection between the size of the Laurentide ice sheet and the orientation of the Atlantic storm track suggests that the ice sheets in North American glacial topography may have influenced the ice sheet evolution in Eurasia. Studies investigating remote climate impacts of the North American and Eurasian paleo-topography typically used static ice sheets as forcing in comprehensive circulation models \citep[e.g.][]{li+battisti2008,lofverstrom_etal2014,ullman_etal2014} or dynamic ice sheet models coupled to highly simplified atmospheric models \citep[sometimes with parameterized climate anomalies][]{beghin_etal2014}. In this study, we investigate the effect of the geologically-constrained ice sheets in North America at MIS5b, MIS4 and LGM (see Fig.\ \ref{fig:kleman}) on the evolution of the Eurasian ice sheet. The atmospheric response to the North American ice sheets is evaluated using a comprehensive atmospheric circulation model with nonlinear dynamics (NCAR CAM3). The atmospheric fields are subsequently used as forcing in a thermomechanical ice-sheet model (SICOPOLIS) in order to evaluate their impact on the Eurasian ice sheet. More information about the models and the experiments is given in Section \ref{sec:models}. In Section \ref{sec:results} we show the main results from the atmospheric and ice-sheet model experiments, followed by a comprehensive discussion in Section \ref{sec:disc}. Finally, the conclusions are summarized in Section \ref{sec:conclusions}.

\section{Models and experiments}
\label{sec:models}

\subsection{Atmospheric simulations}

%\subsubsection{Model description and experiments}
We use the climate snapshot (steady-state) simulations from \cite{lofverstrom_etal2014} representative for the pre-industrial (PI), MIS5b (88 kyrs BP), MIS4 (66 kyrs BP) and LGM (20 kyrs BP) climates. These experiments were conducted with the National Center for Atmospheric Research Community Atmospheric Model version 3 \citep[NCAR CAM3;][]{collins_etal2006} using T85 spectral resolution (approximately 1.4° horizontal resolution) and 26 hybrid levels in the vertical. Ice sheets and other lLand surface processes are handled by the Community Land Model 3 \citep[CLM3;][]{oleson_etal2004}. The ocean surface is represented by a mixed-layer (slab) ocean model with a prescribed mixed-layer depth and ocean heat transport.

For each glacial time slice, we conduct two sets of simulations with different surface topography: two sets of surface orography were used: (i) the reconstructed glacial orographytopography from \cite{kleman_etal2013} (hereafter referred to as the "fullGlacial" simulations; see Fig.\ \ref{fig:kleman}), and (ii) same as (i) except for using present-day topography in North America the present-day orography ("PDoro"hereafter referred to as the ”EAonly” simulations). Each fullGlacial

and PDoro simulation were carried out twice using two end-member representations of the ocean heat transport (OHT). Both OHT representations were derived from equilibrated simulations with the (NCAR) Community Climate System Model version 3 (CCSM3), which is a fully-coupled model using CAM3 as atmospheric component. The first OHT representation was derived from a pre-industrial simulation (hereafter referred to as "PI OHT"), and the second set from the LGM simulation in \cite{brandefelt+otto2009} ("LGM OHT"). The simulations using LGM OHT yield an unrealistically extensive sea-ice cover in the eastern North Atlantic -- reminiscent of the CLIMAP SST reconstruction for LGM \citep{climap1981} -- and hence too cold sea surface conditions compared to proxy data (Fig.\ 1 in the Supplement). Subsequent adjustments of the CLIMAP reconstruction \citep[e.g.][]{paul+schaefer2003,toracinta_etal2004} suggest that the LGM sea-ice margin was located further north in the eastern North Atlantic -- structurally more similar to the one obtained in the simulation with PI OHT (Fig.\ 1 in the Supplement). Therefore, the analyses in this study are mostly based on the simulations with PI OHT, whereas the simulations with LGM OHT are primarily used for sensitivity purposes (Section \ref{sec:disc.oht}).

To evaluate the impact of the North American ice sheet on the Eurasian climate, we carried out six additional simulations with CAM3 specifically for this study. These simulations are identical to the PDoro simulations except that we include only the Eurasian ice sheets but keep the present-day orography elsewhere (hereafter referred to as the "EAonly" simulations). The EAonly simulations are conducted with both OHT parameterizations for all glacial time slices. The impact of the North American ice sheet on the climate is evaluated as the difference between the fullGlacial and EAonly simulations. Note that the influence of the North American ice sheet could also be calculated as the difference between equivalent "NAonly" (simulations with ice sheets in North America but present-day orography elsewhere) and the PDoro simulations. However, such approach is less satisfactory as it would omit feedbacks from the Eurasian ice sheet, and thus most likely inhibit ice growth.

For each time slice, tThe orbital clock \citep{berger+loutre1991} and greenhouse gas concentrations \citep{petit_etal1999,spahni_etal2005} were adjusted to the nominal time of the ice-sheet reconstruction (Table\ \ref{table:ghg}). Other boundary conditions, e.g. aerosols, vegetation , aerosols and landfraction were set to pre-industrial values in all simulations ; the latter two were properly adjusted for glaciated regions \citep{lofverstrom_etal2014}. As reference climate, we use an equilibrated present-day simulation from the same model \citep{hurrell_etal2006}. Results presented below are based on climatologies over 25 years after the simulated climates have reached statistical equilibrium.

\subsubsection{Slab ocean model and ocean heat transport representations}

We use a simplified slab (mixed-layer) ocean model in order to facilitate a high number of experiments, bracketing the uncertainty in the planetary boundary conditions \citep[see also][]{lofverstrom_etal2014}. The slab ocean model has a prognostic sea-surface temperature (SST) calculated from the surface energy balance and the prescribed ocean heat transport (OHT) in the mixed layer \citep{collins_etal2004}. Thus, the slab ocean model does not account for changes in ocean dynamics but retains the thermodynamic feedback between the ocean and the atmosphere.

The westerly mean flow implies that the North Atlantic sea-ice cover has a large influence on the temperature and moisture availability in Eurasia \citep[e.g.][]{smith_etal2003}. The mean position of the North Atlantic sea-ice margin is in turn largely maintained by the Atlantic meridional overturning circulation \citep[AMOC;][]{bitz_etal2005}. The strength of the LGM AMOC is the topic of ongoing research as it cannot be explicitly inferred from proxy-data evidence; modeling studies with coupled atmosphere-ocean models disagree on the LGM AMOC strength with some models suggesting that it was stronger than at present, whereas other models yield a weakening \citep{otto_etal2007,weber_etal2007}. Following \cite{lofverstrom_etal2014}, we therefore use two end-member representations of the OHT to bracket the uncertainty range of the AMOC strength. Both OHT representations are derived from equilibrated simulations with the (NCAR) Community Climate System Model version 3 (CCSM3), which is a fully-coupled model using CAM3 as

atmospheric component. The first OHT representation, which represents a state of a relatively strong AMOC, stems from a pre-industrial simulation (hereafter referred to as "PI OHT"), and the second set — representative for a weak AMOC state — from the LGM simulation in \cite{brandefelt+otto2009} (”BO2009 OHT"). Note that we use the the LGM2 rather than the LGM1 ocean state in \cite{brandefelt+otto2009} because the LGM1 state \citep[originally from][]{otto_etal2006} is not in steady-state \citep{brandefelt+otto2009}. Aside from areas covered by perennial sea ice, simulated changes of the LGM mixed-layer depth are small compared to PI \citep[of order 10 m;][]{brandefelt+otto2009}; following \cite{lofverstrom_etal2014} we therefore use a modern annual mean mixed-layer depth in all simulations.

Changes in the simulated LGM AMOC have a large impact on the sea surface conditions in the North Atlantic; in CCSM3 (CAM3 with BO2009 OHT), the simulated AMOC is reduced with respect to the pre-industrial and the annual mean SSTs are substantially lower than contemporary proxy-based LGM SST reconstructions \citep{margo2009} resulting in a zonal sea-ice margin at $\sim$40°N \citep[Fig.\ \ref{fig:margo}b;][]{brandefelt+otto2009}\footnote{Note that the sea-ice cover in Fig.\ \ref{fig:margo}b is virtually identical to the one obtained in \cite{brandefelt+otto2009} (see their Fig.\ 2), indicating that our slab ocean simulation is consistent with the fully-coupled simulation from which the OHT was derived.}. In CCSM4 \citep[][]{brady_etal2013}, on the other hand, the simulated LGM SSTs are significantly warmer than in CCSM3 and the sea-ice margin is located farther to the north in the eastern North Atlantic \citep[Fig.\ \ref{fig:margo}c;][]{brady_etal2013}, thus in better agreement with LGM sea-ice reconstructions \citep[][]{paul+schaefer2003,toracinta_etal2004,deVernal_etal2005,deVernal_etal2006,margo2009}. We find that the annual mean LGM SST response in CAM3 using PI OHT (Fig.\ \ref{fig:margo}a) is in better agreement with the response in CCSM4 (and thus with the proxy) than in CCSM3. For example, using PI OHT the LGM SST response in the North Atlantic overall has a similar magnitude as suggested by the MARGO data and the sea-ice margin is located further north in the eastern North Atlantic, thus in agreement with the LGM sea-ice reconstructions (Fig.\ \ref{fig:margo}a). Therefore, the analysis in this study is primarily based on the simulations with PI OHT, whereas the simulations with BO2009 OHT are for the most part used for sensitivity purposes (Section \ref{sec:disc.oht}).

\subsection{Ice-sheet model}

\subsubsection{Model description}
To simulate the evolution of the Eurasian ice sheet, we use the three-dimensional ice-sheet model SICOPOLIS (SImulation COde for POLythermal Ice Sheets, version 3.1), which treats ice as an incompressible, viscous and heat-conducting fluid \citep{greve1997}. The model equations are subjected to the shallow-ice approximation, which means that only the lowest order terms are retained \citep{hutter1983}. The model obeys Glen's flow law to calculate strain rates (deformation) from the applied stresses \citep[e.g.][]{van2013}, and a Weertman-type sliding scheme to calculate the basal velocities \citep{weertman1964}. Ice streams are not ~~specifically treated~~explicitly accounted for. We run the model in the "cold-ice mode", i.e.\ temperatures above the pressure melting point are artificially reset to the pressure melting temperature. Expansion of marine ice is allowed if the bathymetry is less than 500 m (default value), otherwise instant calving is assumed. The bedrock and overriding ice sheet are assumed to relax ~~toward~~to isostatic equilibrium with a timescale of 3 kyrs, and the geothermal heat flux is 55 mW m^{-2} over the entire domain.

The surface mass balance is given by the difference between accumulation and ablation. In SICOPOLIS, accumulation is equal to precipitation and the ablation is parameterized using the positive degree day (PDD) approach \citep{braithwaite+olesen1989,reeh1991}. The amount of PDDs in a year is given by the integrated sum of positive temperatures over that year, and is evaluated using the semi-analytical solution in \cite{calov+greve2005}. It is assumed that the daily temperatures in a month are normally distributed about the monthly-mean temperature. The standard deviation (day-to-day variability) of the temperature is 5°C everywhere (default). We use the default values of the degree-day constants, which relate the PDDs to actual melt rates (3 mm day^{-1} K^{-1} for snow and 12 mm day^{-1} K^{-1} for ice). The melting

procedure follows \cite{reeh1991}. First theThe first PDDs are used to melt the annual snow fall. It is assumed that 60$\%$ of that melt water percolates downinto the ice and contributes to the formation of superimposed ice. Second, the superimposed ice is melted, after which the remaining PDDs, if any, are used to melt the glacier ice.

Following \cite{charbit_etal2002} and \cite{charbit_etal2007}, the surface temperature (T) and precipitation (P) over the evolving ice sheet are modified according to a fixed atmospheric lapse rate γ:
\begin{eqnarray}
T (t) &=& T_0 + \gamma (z(t) - z_0), \label{eq:tempsico} \\
P (t) &=& P_0 \exp(\gamma_s \gamma (z(t) - z_0)), \label{eq:precsico}
\end{eqnarray}
where $z(t)$ is the height of the evolving ice-sheet surface ($t=$time), and T_0 and P_0 are the reference temperature and precipitation on the initial ice-free topography z_0, respectively (see Eqs. \ref{eq:tempcorr} and \ref{eq:preccorr} in Section \ref{sec:ism.exp}). Hence, it is assumed that the temperature$T$ decreases linearly with height z at the lapse rate γ (set to value of the standard atmosphere: $\gamma = -6.5 \times 10^{-3}$ K m^{-1}), and that $P $precipitation decreases exponentially with the temperature change (due to elevation) times the parameter γ_s, which relates the temperature anomaly to precipitation change \citep[set to $\gamma_s=0.05$ K^{-1} following][]{charbit_etal2002,charbit_etal2007}. Because the surface temperature on the ice sheet is progressively evolving in time, the relative amount of solid and liquid precipitation is parameterized; following \cite{marsiat1994}, the fraction snowfall to the total precipitation is one if the monthly-mean air temperature is below -10°C, and zero if it is greater than 7°C. For intermediate temperatures the fraction snowfall is linearly interpolated.

\subsubsection{Experimental approachdesign and initial climate forcing}
\label{sec:ism.exp}
The SICOPOLIS simulations are carried out to steady-state (at least 150 kyrs) from an ice-free initial state using the CAM3 simulations as climate forcing. The horizontal resolution is set to 80 km, and the model domain covers most of the Northern Hemisphere. The relatively coarse horizontal resolution is motivated by the fact that we are primarily interested in larger scale first-order changes of the Eurasian ice sheet \cite[as reference,][used a horizontal resolution of 95 km in their ice-sheet reconstructions]{kleman_etal2013}. The vertical resolution amounts to 81 levels in the ice and 11 levels in the bedrock.

We use the procedure described in \cite{charbit_etal2007} to deduce the initial fields of surface temperature (T_0) and precipitation (P_0) from the atmospheric model:
\begin{eqnarray}
T_0 &=& T_{PD,obs} + T_{paleo,CAM} - T_{PD,CAM} - \gamma (z_{paleo} - z_{PD}),
\label{eq:tempcorr} \\
P_0 &=& P_{PD,obs} \times (P_{paleo,CAM} / P_{PD,CAM}) \times \exp[-\gamma_s \gamma (z_{paleo} - z_{PD})]. \label{eq:preccorr}
\end{eqnarray}
To account for systematic biases in the atmospheric modelclimatology we first calculate anomalies of the glacial temperature ($T_{paleo,CAM}$) with respect to the temperature of the present-day simulation ($T_{PD,CAM}$). In doing so, we correct for the different orographies in the glacial and present-day simulations ($z_{paleo,CAM}$ and $z_{PD,CAM}$, respectively) using the standard lapse rate. Subsequently, the anomalies are bi-linearly interpolated to the SICOPOLIS grid and added to the observational dataset ($T_{PD,obs}$), which is based on ERA -Intirim Intirim reanalysis data \citep{dee_etal2011}. To calculate P_0 we use the same technique as for T_0, but we use ratios instead of anomalies in order to avoidomit negative precipitation \citep{charbit_etal2007}.

\section{Results}
\label{sec:results}

\subsection{Atmospheric response}

\subsubsection{Summer temperature}
The annual ablation is dominated by the summer conditions; we therefore focus on the surface temperature in boreal summer (June--August: JJA). Figure\ 2 shows the JJA surface temperature in the ~~ERA-Interim \citep{dee_etal2011}~~ reanalysis data (a), present-day simulation (b) and the EAonly paleo simulations (c,e,g). To highlight areas susceptible~~-~~ for inception, the temperatures in Fig.\ \ref{fig:temp} are projected to the present-day orography using the standard lapse rate. A summary of the average summer temperatures in the Northern Hemisphere and Eurasia is presented in Table\ \ref{table:temp}.

The average Northern Hemisphere summer temperature decreases across the EAonly simulations; it drops by 3°C between present-day and MIS5b, and by an additional 2°C at LGM (Table\ \ref{table:temp}). The ~~progressive~~ cooling across the glacial simulations has even larger regional variations: in Eurasia, the LGM summer temperature is about 5°C lower than at MIS5b (Table\ \ref{table:temp}). Regions with sub-freezing summer temperatures are particularly interesting for glacial inception~~; --~~ the average position of the zero-degree summer (surface) isotherm in indicated by the green contour in Fig.\ \ref{fig:temp}a,b,c,e,g. Similar to present-day (Fig.\ \ref{fig:temp}a,b), the zero-degree isotherm at MIS5b is mainly located in the Arctic Ocean poleward of the Eurasian continent (Fig.\ \ref{fig:temp}c). Owing to the cooler conditions at MIS4 and LGM, the (zonal) average location of the zero-degree isotherm is shifted equatorward by ~~approximately~~ 6 to 7° ~~equatorward~~ (Table\ \ref{table:temp}); the largest regional changes are found in Scandinavia and eastern Siberia, where it reaches as far south as 60°N at MIS4 and LGM (Fig.\ \ref{fig:temp}e,g).

Figure\ \ref{fig:temp}d,f,h shows the summer (surface) temperature anomalies induced by the North American ice sheet. These anomalies are calculated as the difference between the fullGlacial and EAonly simulations; a lapse rate correction has been applied to account for elevation differences. Due to an increased surface albedo and cold air advection by orographically~~-~~ forced stationary waves \citep{cook+held1988,roe+lindzen2001,abe-ouchi_etal2007,liakka+nilsson2010,liakka2012,lofverstrom_etal2015}, the largest cooling occurs in the vicinity of the North American ice sheet. In Eurasia, the temperature response to the North American ice sheet exhibits large regional variations. For all time slices, the North American ice sheet induces colder conditions in Europe~~, whereas. T~~the response in Siberia is more complicated; at MIS5b the Siberian temperature response is almost negligible (Fig.\ \ref{fig:temp}d), whereas there is a warming in eastern Siberia at MIS4 and LGM. The largest difference between the MIS4 and LGM responses is found in central Siberia, which becomes colder~~is cooler~~ at MIS4 (Fig.\ \ref{fig:temp}f) and warmer at LGM (Fig.\ \ref{fig:temp}h).

\subsubsection{Annual precipitation}
The large-scale features of the annual precipitation in the EAonly simulations are reminiscent of the modern climate, although the global precipitation rates are somewhat reduced in the glacial simulations (Fig.\ \ref{fig:precip}a,b,c,e,g). The largest precipitation rates in Eurasia are found in northwestern Europe where the cyclones from the Atlantic stormtrack make landfall.

As for the temperature, the largest precipitation response to the North American ice sheet is found ~~locally~~over the ice sheet itself, with generally increased precipitation on the windward (westerly) slopes of the ice sheet and reduced precipitation over the leeward (easterly) slopes (Fig.\ \ref{fig:precip}d,f,h). In Eurasia, the North American ice sheet has a relatively small impact on the precipitation at MIS5b and MIS4 (Fig.\ \ref{fig:precip}d,f), but yields a significantly reduced precipitation in northwestern Europe at LGM (Fig.\ \ref{fig:precip}h). As discussed in \cite{lofverstrom_etal2014}, the reduced precipitation rates at LGM is associated with a zonalisation of the midlatitude Atlantic jet stream resulting from flow-topography interactions with the continent-wide North American ice sheet ~~at LGM~~ \citep[][]{li+battisti2008,ullman_etal2014,merz_etal2015, pausata+lofverstrom2015}. \cite{lofverstrom_etal2014} found that this effect is not present for the smaller pre-LGM ice sheets

(MIS5b and MIS4), as their location and spatial extent allow the mean-flow to largely circumvent the topography, thus rendering the tilt of the Atlantic jet -- and stormtrack -- largely similar to the present-day.

\subsubsection{Summer stationary waves}
\label{sec:res.waves}

~~To gain some insight into~~In order to understand the temperature response in Fig.\ \ref{fig:temp}, we examine the stationary Rossby waves in the different climate states. Stationary waves, defined as zonal asymmetries in the climatological fields, are the result of large scale orography and diabatic heating \citep[e.g.][]{hoskins+karoly1981,held_etal2002,held1983,kaspi+schneider2011}. Ice sheets constitute both orographic and diabatic forcing of stationary waves. Therefore, ice sheets expanding into the westerly mean flow can potentially influence the global stationary wave field \citep[e.g.][]{cook+held1988,roe+lindzen2001,lofverstrom_etal2014}.

The lower troposphere (700 hPa) geopotential height anomalies from the EAonly simulations are shown in Fig.\ \ref{fig:z}c,e,g. The stationary wave response is qualitatively similar in all glacial time slices; similar to the modern climate (Fig.\ \ref{fig:z}a,b), the summer stationary wave field is characterized by anticyclonic circulation (ridges) over the subtropical Pacific and Atlantic ocean basins, and cyclonic circulation (troughs) over Asia and northeastern Canada (Fig.\ \ref{fig:z}c,e,g). In addition, the ridge over the Atlantic Ocean extends over Europe and covers most of the ice sheet area, suggesting that the local ridge is excited by the Eurasian ice sheet. As noted by \cite{lofverstrom_etal2014}, this indicates that the ice sheet'âs diabatic cooling is dominating the stationary wave response.

The 700 hPa geopotential height responses to the North American ice sheets are shown as shading in Fig.\ \ref{fig:z}d,f,h. As expected from theory, the stationary wave amplitudes increases with the size (spatial extent and height) of the North American ice sheet \citep[][]{cook+held1992,ringler+cook1997,liakka+nilsson2010,liakka_etal2011,lofverstrom_etal2014}. Besides the amplitude, the stationary wave response to the North American ice sheet is qualitatively similar in all time slices. The local response is a ridge over the northwestern parts of the North American ice sheet and a trough in the southeast. This particular response is a robust feature across models using nonlinear stationary wave dynamics \citep{ringler+cook1997,ringler+cook1999,liakka_etal2011}. The remote downstream response consists of two wavetrains: (i) a subtropical wavetrain with a northwest-southeast orientation, and (ii) a low wavenumber polar wavetrain with a more zonal orientation. The polar wavetrain is characterized by a trough over Europe/western Asia and a ridge over Siberia.

The contours in Fig.\ \ref{fig:z}d,f,h depict the geopotential height anomalies at 300 hPa. ~~Note that t~~The anomalies at this level have essentially the same spatial location as at 700 hPa, indicating that the climatological response to the North American ice sheet is largely equivalent barotropic.

In the summer season, high-latitude geopotential height anomalies are typically well correlated with surface temperature anomalies ~~of the surface temperature~~. Ridges are associated with reduced cloudiness and increased downwelling shortwave radiation, which leads to a surface warming, whereas troughs typically yield increased cloudiness and thus lower surface temperatures. This is also seen here (cf.\ Fig.\ \ref{fig:temp}d,f,h and \ref{fig:z}d,f,h): the ridge over eastern Siberia and Alaska is associated with a surface warming, and the trough in Europe with ~~colder conditions~~a cooling. Note that the magnitude of these temperature anomalies, in particular the Siberian warm anomaly, is not only controlled by the geopotential height anomalies, but also by albedo feedbacks due to changes in the snow cover (see Fig.\ ~~1~~2 in the Supplement).

\subsection{Ice-sheet evolution}
In this section we examine how the altered climate conditions -- induced by the North American ice sheet -- influence the spatial equilibrium extent of the Eurasian ice sheet. To evaluate our results, we compare the simulated extents of the Eurasian ice sheet with the geologically-constrained

reconstructions from \cite{kleman_etal2013}. Note that we only compare the geographical distribution of ice (i.e.\ ice area), but not the ice thickness or ice volume. The reason is that the ice thickness in the \cite{kleman_etal2013} reconstructions is a model dependent feature, whereas the spatial extents are constrained by geological evidence.

Figure\ \ref{fig:h} shows the simulated equilibrium ice thickness when using the atmospheric simulations summarized in Figs.\ \ref{fig:temp} and \ref{fig:precip} as climate forcing. Apart from some ice caps in the Scandinavian mountains, Eurasia remains ~~virtually~~ ice free at MIS5b (Fig.\ \ref{fig:h}a,b). This is consistent with a negative surface mass balance over essentially the entire domain (Fig.\ ~~23~~ in the Supplement). A comprehensive discussion on the potential shortcomings in the MIS5b simulations follows in section \ref{sec:disc.mis5b}.

At MIS4 and LGM, atmospheric circulation changes induced by the North American ice sheet serves to increase the total ice area in Eurasia by about 80$\%$ and 30$\%$, respectively (Fig.\ \ref{fig:h}). This increase is mediated by an expansion of ice in ~~Europe~~western Eurasia and a reduced ice extent in eastern Siberia; apart from ~~somewhat~~slightly too much ice in the Kara-sea region in the LGM simulation, the outlines of the simulated MIS4 and LGM ice sheets in Eurasia are in good agreement with the reconstructions from \cite{svendsen_etal2004} and \cite{kleman_etal2013}; see ~~(~~Fig.\ \ref{fig:h}d,f~~)~~. In the absence of ice in North America, the MIS4 and LGM ice sheets are ~~fairly~~more zonally distributed along the Arctic coast (Fig.\ \ref{fig:h}c,e). Hence, our simulations suggest that the North American ice sheet induces a westward migration of the Eurasian ice sheet, and consequently,~~; as a result~~ the evolution of the Eurasian ice sheet between MIS4 and LGM was to a large extent controlled by the growth of the North American ice sheet.

The ice sheet~~'â~~s westward migration is ~~elucidated~~depicted in Fig.\ \ref{fig:center}, which shows the longitude of the center of mass (λ_c) of the total ice distribution in Eurasia. In the reconstructions from \cite{kleman_etal2013}, λ_c decreases from 49°E at MIS5b to 44°E and 27°E at MIS4 and LGM, respectively (black bars in Fig.\ \ref{fig:center}). Note that the westward migration between MIS4 and LGM is captured only if the North American ice sheet is present (white bars in Fig.\ \ref{fig:center}), otherwise λ_c remains large ($\sim$55-60°E) for both stages (grey bar~~y~~s in Fig.\ \ref{fig:center}).

\section{Discussion}
\label{sec:disc}

We have examined how the North American ice sheet (constrained by geological data) influences the extent of the Eurasian ice sheet in the MIS5b, MIS4 and LGM climate states. We found that the MIS4 and LGM ice sheets in North America yield a westward migration of the Eurasian ice sheet (Fig.\ \ref{fig:center}), characterized by more ice in Europe and less ice in Siberia (Fig.\ \ref{fig:h}). ~~In the presence of~~When accounting for the North American ice sheet, the spatial distributions of the simulated MIS4 and LGM ice sheets in Eurasia are in good agreement with contemporary ice-sheet reconstructions \citep[Fig.\ \ref{fig:h};][]{svendsen_etal2004,kleman_etal2013}; this suggests that the growth of the North American ice sheet between MIS4 and LGM may have been vital for limiting and shifting ~~the westward migration of~~ the Eurasian ice sheet ~~during this time.~~westward in time.

\subsection{North American influence on the Eurasian climate}

The westward migration of the Eurasian ice sheet in the MIS4 and LGM simulations (Figs.\ \ref{fig:h} and \ref{fig:center}) is associated with changes in the summer stationary wave field. The North American ice sheet yields a cooling (less ablation) in Europe and a warming (more ablation) in northeastern Siberia (Fig.\ \ref{fig:temp}f,h). These temperature anomalies are associated with an equivalent barotropic cyclonic/anticyclonic anomaly in the target regions; this is particularly true for the low wavenumber anomalies at high latitudes (Fig.\ \ref{fig:z}f,h).

The geopotential height anomalies in Fig.\ \ref{fig:z}d,f,h result from (typically nonlinear) interactions between the atmospheric flow and the thermal and orographic forcing of the North American ice sheet. This typically leads to a complicated nonlinear response in the vicinity of the wave source (i.e. the North American ice sheet in our case) where the climate anomalies rotate clockwise for larger topographic barriers \citep{held+cook1992,ringler +cook1997,liakka_etal2011,liakka2012}. Away from the wave source, however, the geopotential height anomalies share many similarities with linear wave theory (see Appendix A for details). For example, the low wavenumber polar wave train in Fig.\ \ref{fig:z}d,f,h is consistent with a latitudinal decrease of the (barotropic) stationary wavenumber due to the spherical geometry of the planet (Appendix A and Fig.\ 3 in the Supplement). In addition, linear Rossby wave tracing arguments \citep[Appendix A and][]{hoskins+karoly1981} suggest that higher latitude wave trains should have a more zonal orientation than wave trains at lower latitudes, thus consistent with Fig.\ \ref{fig:z} d,f,h.

Although the remote stationary wave response is broadly consistent with linear theory, our findings are different from the coupled ice sheet-climate model experiments \cite{beghin_etal2014}, who used CLIMBER-2 with (linear) parameterized stationary waves to examine the interdependence between the Northern Hemisphere ice sheets. They found that the North American ice sheet has a negligible impact in European summer temperatures but yields a slight cooling in Siberia, thus contradicting our results (Fig.\ \ref{fig:temp}). Although CLIMBER has proven to be a valuable model for studying the transient ice sheet-climate evolution through the glacial cycles \citep[e.g.][] {calov_etal2002,calov_etal2005,bonelli_etal2009,ganopolski_etal2010,ganopolski+calov2011}, it has a very limited representation of the atmospheric circulation; in particular it does not account for Rossby wave dynamics. Unless explicitly corrected for \citep{ganopolski_etal2010}, the lack of Rossby wave dynamics in CLIMBER typically facilitates ice inception over the western rather than the eastern part of North America \citep{bonelli_etal2009,beghin_etal2014}; this presumably influenced the Eurasian climate anomalies in \cite{beghin_etal2014}.~~–~~

~~The discussion is divided into three parts. First, in Section \ref{sec:disc.west} we analyse the stationary wave response to the North American ice sheet -- and the associated westward migration of Eurasian ice sheet -- from a theoretical perspective by employing linear theory. Second, because the simulated ice sheets presented thus far have been based on atmospheric simulations with a constant (pre-industrial) OHT, we investigate the sensitivity of our results to the OHT in Section\ \ref{sec:disc.oht}. This exercise is particularly relevant because of the large uncertainty associated with changes of the Atlantic Meridional Overturning Circulation (AMOC) in glacial climates \citep{weber_etal2007}. Finally, in Section\ \ref{sec:disc.mis5b}, potential reasons for the lack of ice growth in our MIS5b experiment are discussed. Since the simulated MIS4 and LGM ice extents -- that are in agreement with the data-based reconstructions -- were obtained using essentially the default parameters in SICOPOLIS, we will not explore the entire parameter space of the model to induce ice-sheet inception for MIS5b. Instead, the discussion focuses on potential issues with the experimental approach.~~

~~\subsection{Westward migration of the Eurasian ice sheet} \label{sec:disc.west}~~

~~The westward migration of the Eurasian ice sheet in the MIS4 and LGM simulations (Figs.\ \ref{fig:h} and \ref{fig:center}) is associated with changes in the summer stationary wave field. It is found that the North American ice sheet yields a cooling (less ablation) in Europe and a warming (more ablation) in northeastern Siberia (Fig.\ \ref{fig:temp}f,h). These temperature anomalies are associated with an equivalent barotropic cyclonic/anticyclonic structure in the target regions; this is particularly true for the low wavenumber anomalies at high latitudes (Fig.\ \ref{fig:z}f,h). For example, the more westward location of the Siberian warm anomaly at the LGM than at MIS4 is associated with a more westward extent of the Siberian ridge.~~

~~The height anomalies in Fig.\ \ref{fig:z}d,f,h result from (typically nonlinear) interactions between the atmospheric flow and the thermal and orographic forcing of the North American ice sheet. Due~~

to the complexity of the atmospheric model, it is useful to resort to simpler linear models to gain a conceptual understanding of the stationary wave field. Linear models have been shown to qualitatively capture the large-scale features of the stationary waves in the present-day atmosphere \citep{charney+eliassen1949,held1983,held_etal2002}. However, many features omitted in linear models, such as zonal variations in the background state and (nonlinear) wave-wave interactions can significantly alter the stationary wave response \citep[e.g.][]{cook+held1992,hoskins+ambrizzi1993,ringler+cook1997}. Therefore, results from linear models should only be considered as a qualitative first-order estimate of the total wave response. The equivalent barotropic structure in Fig.\ \ref{fig:z}d,f,h suggests that the stationary wave response to the North American ice sheet is dominated by orographic rather than thermal forcing; the latter has been shown to yield stationary waves with a more baroclinic structure \citep[height anomalies tilt westward with altitude][]{hoskins+karoly1981,ting1994,ringler+cook1999}. Therefore, we use the linear barotropic model in spherical geometry with orographic forcing to analyse the wave response. This is the simplest model that can be used to study meridional dispersion of stationary waves \citep{held1983}. In particular, the linear Rossby wave ray tracing theory provided in \cite{hoskins+karoly1981} is useful for analysing the disposition of stationary wavetrains.

In models linearized about a zonal mean basic state, the horizontal scale of the stationary waves is given by the "stationary wavenumber" K_s, which is a function of the atmospheric background state. In the barotropic model, K_s is given by \citep{held1983}:

\begin{equation}
K_s^2 = k^2 + l^2 = \cos^2 \phi \left(\frac{\beta + a^{-1} \partial [\zeta] / \partial \phi}{[u]} \right),
\label{eq:ks}
\end{equation}

where β and $a^{-1} \partial [\zeta] / \partial \phi$ are the meridional gradients of planetary and (zonal mean) relative vorticity, $[u]$ is the zonal mean background flow, ϕ the latitude and k and l denote zonal and meridional wavenumbers, respectively. In the present-day atmosphere \citep{hoskins+karoly1981,held1983} as well as in our simulations (Fig.\ \ref{fig:ks}), K_s is a monotonically decreasing with latitude (as β and $cos(\phi) \rightarrow 0$ towards the pole). This implies that stationary waves at high latitudes typically have lower zonal wavenumbers than those propagating at lower latitudes. Hence, the low wavenumber response at high latitudes in Fig.\ \ref{fig:z}d,f,h ($>60^\circ$N) is essentially a result of the small K_s due to the spherical geometry of the planet.

Following \cite{hoskins+karoly1981}, the propagation direction of stationary waves is given by the direction of the local group velocity: $\mathbf{c_g} = (c_{gx}\mathbf{i},c_{gy}\mathbf{j})$. Because c_{gy} is identical to c_{gx} except for a factor l instead of a k\footnote{For stationary waves, $c_{gx}=2\beta k^2 / (k^2 + l^2)^2$ and $c_{gy}=2\beta kl / (k^2 + l^2)^2$. Hence, $c_{gx} >0$, which implies that the wave energy always propagates eastward. c_{gy}, on the other hand, depends on the sign of l, which corresponds to poleward (positive l) and equatorward (negative l) propagation.} \citep{hoskins+karoly1981,vallis2006}, the inclination (α) of the ray path (propagation direction) is given by:

\begin{equation}
\tan \alpha = \frac{c_{gy}}{c_{gx}} = \frac{l}{k}.
\label{eq:incl}
\end{equation}

Here, k is constant along a ray; hence as K_s decreases with latitude (Fig.\ \ref{fig:ks}), $|l|$ must decrease to satisfy Eq.\ \ref{eq:ks}. This implies that waves at high latitudes propagate along more zonal paths than waves at lower latitudes (Eq.\ \ref{eq:incl}); this is seen also in Fig.\ \ref{fig:z}d,f,h, where the polar wavetrain is more zonally oriented than the subtropical wavetrain. Hence, despite the high complexity of the atmospheric circulation model used here, the key features (wavenumber and orientation) of the polar wavetrain in Fig.\ \ref{fig:z}d,f,h -- that are associated with the westward migration of the Eurasian ice sheet -- are consistent with linear barotropic theory. This suggests that simplified atmospheric circulation models, which capture the fundamental dynamics, can be used to study teleconnections between the North American and Eurasian ice sheets.

\subsection{Sensitivity to OHT}
\label{sec:disc.oht}

~~One of the main drawbacks with the model setup used in this study is that it does not have an interactive dynamic ocean model that responds to changes in the atmospheric circulation. For the Eurasian climate, changes in the Atlantic meridional overturning circulation (AMOC) are particularly important as it transports warm surface water poleward and thereby influences the mean position of the sea-ice margin in the North Atlantic \citep{bitz_etal2005}.~~
~~The strength of AMOC during glacial times is highly model dependent; for the LGM some of the coupled atmosphere-ocean models in the Paleomodeling Intercomparison Project (PMIP) yield a strengthening of the AMOC compared to present-day whereas others yield a weakening \citep{otto_etal2007,weber_etal2007}. In addition, results diverge within the same model family; CCSM3 exhibits a general weakening of the AMOC for LGM, ultimately ending up with the "CLIMAP-like" sea-ice cover in \cite{brandefelt+otto2009} (LGM OHT in Supplementary Fig.\ 1), whereas the more recent model CCSM4 yields a slightly increased AMOC \citep{brady_etal2013}.~~

Owing to the large uncertainty of the AMOC response during glacial times \citep{otto_etal2007,weber_etal2007}, we perform sensitivity simulations of the equilibrium ice thickness using the atmospheric simulations with ~~the~~BO2009 OHT ~~derived from~~ \citep{brandefelt+otto2009} ~~(LGM OHT)~~ as climate forcing. The results are summarized in Fig.\ \ref{fig:h_q2}. Due to the colder conditions in the simulations with ~~LGM~~BO2009 OHT, the Eurasian ice sheet expands equatorward compared to when using PI OHT (cf.\ Fig.\ \ref{fig:h_q2} and \ref{fig:h}). Notably, however, despite the colder conditions in the North Atlantic, the model fails to simulate a ~~sufficiently~~ large ice sheet ~~for~~at MIS5b (Fig.\ \ref{fig:h_q2}a,b). ~~Compared to the PI OHT simulations, the MIS4 and LGM ice sheets are significantly larger in the LGM OHT simulations (Fig.\ \ref{fig:h_q2}c-f).~~

Using the BO2009 OHT climate forcing, ~~T~~the North American ice sheet ~~yields~~induces a westward migration of the Eurasian ice sheet ~~also in the LGM OHT simulations~~ (λ_c is reduced by 6° for MIS4 and by 11° for LGM; not shown); however, it is not as pronounced as ~~in~~with ~~the~~ PI OHT ~~simulations~~ (Fig.\ \ref{fig:center}). ~~Because~~Since the climate response to the North American ice sheet is qualitatively similar in the ~~LGM~~BO2009 OHT (Figs.\ 4, 5 and 6 in the Supplement) and the PI OHT simulations (Figs.\ \ref{fig:temp}, \ref{fig:precip} and \ref{fig:z}), the reduced westward migration in the ~~LGM~~BO2009 OHT simulations is most likely attributed to ~~the~~a colder climate; in the PDD model, cold background conditions (temperatures below freezing) reduces the effect of temperature anomalies on the ablation.

\subsection{What prevents ice-sheet growth at MIS5b?}
\label{sec:disc.mis5b}

The vexing issue of this study is that we fail to simulate a MIS5b ice sheet of comparable size to the data-based reconstructions (Fig~~s~~.\ \ref{fig:h} and \ref{fig:h_q2}) ~~-- even when using the colder LGM OHT climate conditions (Fig.\ \ref{fig:h_q2})~~. The lack of ice growth at MIS5b is associated with a negative surface mass balance across the entire Eurasian continent (Fig.\ ~~23~~ in the Supplement) due to relatively high summer temperatures (Fig.\ \ref{fig:temp} and Table\ \ref{table:temp}). The relatively warm conditions at MIS5b compared to MIS4 and LGM are attributed ~~to~~ both to a higher insolation and higher concentrations of greenhouse gases ~~concentrations~~ (Table\ \ref{table:ghg}). It is possible that allowing for certain feedbacks, such as vegetation changes \citep{colleoni_etal2009,liakka_etal2014}, would cool the summer climate and thus support ice inception at MIS5b. However, because the MIS4 and LGM extents of the Eurasian ice sheets are in good agreement with the reconstructions when omitting these feedbacks, it seems unlikely that systematic biases in the climate forcing is the primary cause for the lack of ice growth at MIS5b.

~~Possibly, missing processes in the ice-sheet model inhibit the early development of ice sheets. For example, SICOPOLIS does not treat ice streams so there is no use of the shallow-shelf approximation \citep[SSA;][]{macayeal1989}; this considerably reduces the basal velocities \citep{macayeal1989}. Under relatively warm conditions (such as MIS5b), the use of SSA could trigger higher velocities in some areas and thereby cause a faster expansion of the ice sheet. The faster ice expansion, along with the ensuing temperature-elevation feedback, could in some cases compensate for a negative surface mass balance and thus support ice-sheet inception.~~

~~However, the most obvious caveats are associated with the setup of our experiments., . All the ice-sheet model simulations conducted here were integrated to equilibrium starting from ice-free (bare ground) conditions. The good agreement between the simulated MIS4 and LGM extents and the proxy suggests that these ice sheets were essentially in equilibrium with the prevailing climate; this is, however, not necessarily true for MIS5b. Instead, it is plausible that the MIS5b ice sheet is a remnant of preceding ice-sheet configurations and climate conditions. In this context it is interesting to note that the Eurasian ice sheet reached a size comparable to MIS5b already at $ \sim$105 kyrs BP, subsequent to a relative minimum in the high-latitude boreal summer insolation \citep{kleman_etal2013,lofverstrom_etal2014}.~~
In addition, we fail to find multiple equilibrium states \citep[e.g.][]{calov+ganopolski2005,abe-ouchi_etal2013} of the simulated Eurasian ice sheets (Fig.\ 7 in the Supplement); initializing the ice-sheet simulations using the \cite{kleman_etal2013} reconstructions leads to very similar equilibrium extents as in Fig.\ \ref{fig:h}. This suggests that preceding configurations of the Eurasian ice sheet were not crucial for maintaining the ice sheet at MIS5b.

Instead, it is more likely that the MIS5b ice sheet was not in equilibrium with the prevailing climate. The successful glacial inception and good agreement between the equilibrated MIS4 and LGM ice sheets and the reconstructions suggests that the climate was locally cold enough to support glacial inception and the resulting ice sheets were in equilibrium with the prevailing climate; this is, however, not necessarily true for MIS5b. Instead, it is plausible that the MIS5b climate was too warm to support glacial inception and the ice sheet was a remnant of ice growth in preceding colder periods. In this context it is interesting to note that the Eurasian ice sheet reached a size comparable to MIS5b already at $\sim$105 kyrs BP, subsequent to a relative minimum in the high-latitude boreal summer insolation \citep{kleman_etal2013,lofverstrom_etal2014}.

~~In order to test the effect of the ice-sheet and climate history on the extent of the MIS5b ice sheet, we conduct two sensitivity experiments in SICOPOLIS. In the first experiment, we use the \cite{kleman_etal2013} reconstruction in Eurasia (Fig.\ \ref{fig:kleman}a) instead of an ice-free state as initial condition. Initializing the model with a pre-existing ice sheet yields lower initial temperatures on the ice sheet (due to the atmospheric lapse rate) than with bare ground. In the simulations initialized with the \cite{kleman_etal2013} reconstruction, the ice extent increases slightly in the Barents sea region compared to the simulations initiated from an ice-free state (Fig.\ \ref{fig:h_mis5b}a,b). Aside from that, however, Eurasia remains predominately ice-free also when using the reconstructed ice sheet as initial condition.~~

~~In the second experiment we test the sensitivity of the extent of the MIS5b ice sheet to the colder climate history. Because~~Since we do not have access to any atmospheric simulations of a colder stages prior to MIS5b, we use a crude approach by imposing a cooling of the JJA temperature artificially in SICOPOLIS. To estimate the magnitude of the cooling, we employ the parameterization of the surface temperature to changing insolation ~~in~~proposed by \cite{abe-ouchi_etal2007,abe-ouchi_etal2013}; based on sensitivity experiments with a coupled atmosphere-ocean model, they obtained a linear relationship between changes of the high-latitude temperature (ΔT_{insol}) and insolation (ΔQ): $\Delta T_{insol} = 3.25 \times \Delta Q / 40$. The insolation at the youngest minimum preceding MIS5b (at $\sim$95 kyrs BP) was about 40 W m $^{-2}$ lower than at MIS5b \citep{berger+loutre1991}; this yields $\Delta T_{insol} \approx -3^\circ$C. Using the colder "minimum insolation" conditions, the extent of the Eurasian ice sheet agrees well with the MIS5b reconstruction in Scandinavia and the Barents sea region (Fig.\ \ref{fig:h_mis5b}~~ac~~,~~bd~~) -- in particular when the North American ice sheet is included (Fig.\

\ref{fig:h_mis5b}bd) -- whereas the Kara sea region continually remains ice free. Hence, in contrast to MIS4 and LGM, our first-order sensitivity analysis suggests that the MIS5b extent of the Eurasian ice sheet is predominately a resultresults as a memory of preceding colder stages rather than the prevailing climate.

\conclusions
\label{sec:conclusions}
We have examined the impact of the geologically-constrained MIS5b, MIS4 and LGM ice sheets in North America on the spatial extent of the Eurasian ice sheet. The conclusions are summarized as follows:

\begin{itemize}
\item[--] The North American ice sheet yields a cooler summer temperatures in Europe and warmer temperatures in northeastern Siberia in all time slices. The amplitude of these anomalies and the westward extent of the Siberian warming increase with the size of the North American ice sheet (Fig.\ \ref{fig:temp}).

\item[--] The temperature anomalies are associated with an equivalent barotropic cyclonice and anticyclonic anomalye in Europe and Siberia, respectively (Fig.\ \ref{fig:z}). The structure of the circulation anomalies away from the wave forcing is qualitatively consistent with linear barotropic stationary wave theory.

\item[--] Owing to its impact on the Eurasian summer temperatures, the North American ice sheet controls the westward migration of the Eurasian ice sheet; in the presence of the North American ice sheet, the spatial extents of the simulated Eurasian ice sheets at MIS4 and LGM are consistent with contemporary ice-sheet reconstructions \citep{svendsen_etal2004,kleman_etal2013}. However, if the North American ice sheet is omitted, the Eurasian ice sheet becomes more zonally distributed with a more eastward located center of mass (Figs.\ \ref{fig:h}, \ref{fig:center}).

The stationary wave response to the North American glacial topography is not that sensitive to changes in the ocean heat transport (compare Figs.\ \ref{fig:temp} and \ref{fig:z} with Figs.\ 4 and 6 in the Supplement). Nevertheless, a weakening of AMOC reduces the influence of the North American glacial topography on the Eurasian ice-sheet evolution by imposing cooler background conditions in Eurasia (Fig.\ \ref{fig:h_q2}).

\item[--] Although the spatial extents of the MIS4 and LGM ice sheets are well captured by SICOPOLIS, Eurasia remains essentially ice free for MIS5b. Unlike MIS4 and LGM, first-order sensitivity analysis reveals that the MIS5b ice sheet was not in equilibrium with the prevailing climate, but mostmore likely a result of preceding colder climate conditions.

\item[--] Our study suggests that the westward migration of the Eurasian ice sheet between MIS4 and LGM was induced by the expansion of the North American ice sheet. Furthermore, our results areis consistent with the notion that the east-heavy Eurasian ice sheet at the late Saalian Maximum ($\sim$140 kyrs BP) was accompanied by a relatively small ice sheet in North America \citep{svendsen_etal2004,colleoni_etal2014}.

\end{itemize}

\appendix
\section{}

Due to the complexity of the atmospheric model, it is useful to resort to a simpler linear framework to obtain a conceptual understanding of the stationary wave field. Linear models have been shown to qualitatively capture the large-scale features of the stationary waves in the present-day atmosphere \citep{charney+eliassen1949,held1983,held_etal2002}. However, many features omitted in linear models (e.g.\ zonal variations in the background state and nonlinear interactions

between different forcing agents) can significantly alter the stationary wave response \citep[e.g.][]{cook+held1992,hoskins+ambrizzi1993,ringler+cook1997}. Therefore, results from linear models should only be considered as a qualitative first-order estimate of the total wave response. The equivalent barotropic structure in Fig.\ \ref{fig:z}d,f,h suggests that the wave field is dominated by orographic rather than thermal forcing; the latter has been shown to yield stationary waves with a more baroclinic structure \citep[geopotential height anomalies tilt westward with altitude][]{hoskins+karoly1981,ting1994,ringler+cook1999}. Therefore, we use the orographically forced linear barotropic model \citep[this is the simplest model that can be used to study meridional dispersion of stationary waves;][]\citep{held1983}.

In models linearized about a zonal mean basic state, the horizontal scale of the stationary waves is given by the "stationary wavenumber" K_s, which is a function of the atmospheric background state. In a barotropic model, K_s is given by \citep{held1983}:
\begin{equation}
K_s^2 = k^2 + l^2 = \cos^2 \phi \left(\frac{\beta + a^{-1} \partial [\zeta] / \partial \phi}{[u]} \right),
\label{eq:ks}
\end{equation}
where β and $a^{-1} \partial [\zeta] / \partial \phi$ are the meridional gradients of planetary and (zonal mean) relative vorticity, $[u]$ is the zonal mean background flow, ϕ the latitude and k and l denote zonal and meridional wavenumbers, respectively. In the present-day atmosphere \citep{hoskins+karoly1981,held1983} as well as in our simulations (Fig.\ 3 in the Supplement), K_s is monotonically decreasing with latitude (as β \sim $cos(\phi) \rightarrow 0$ toward the pole). This implies that stationary waves at high latitudes typically have lower zonal wavenumbers than those propagating at lower latitudes. Hence, the low wavenumber response (small K_s) at high latitudes in Fig.\ \ref{fig:z}d,f,h ($>60^\circ$N) is essentially a result of spherical geometry of the planet.

Following \cite{hoskins+karoly1981}, the propagation direction of stationary waves is given by the direction of the local group velocity (in the limit of WKB): $\mathbf{c_g} = (c_{gx}\mathbf{i},c_{gy}\mathbf{j})$. Because c_{gy} is identical to c_{gx} except for a factor l instead of k \citep{hoskins+karoly1981,vallis2006}\footnote{For stationary waves, $c_{gx}=2\beta k^2 / (k^2 + l^2)^2$ and $c_{gy}=2\beta kl / (k^2 + l^2)^2$. Hence, $c_{gx}>0$, which implies that the wave energy always propagates eastward. c_{gy}, on the other hand, depends on the sign of l, which corresponds to poleward (positive l) and equatorward (negative l) propagation.}, the inclination (α) of the ray path (propagation direction) is given by:
\begin{equation}
\tan \alpha = \frac{c_{gy}}{c_{gx}} = \frac{l}{k}.
\label{eq:incl}
\end{equation}
Here, k is constant along a ray; hence as K_s decreases with latitude (Fig.\ 3 in the Supplement), $|l|$ must decrease to satisfy Eq.\ \ref{eq:ks}. This implies that waves at high latitudes propagate along more zonal paths than waves at lower latitudes (Eq.\ \ref{eq:incl}); this is seen also in Fig.\ \ref{fig:z}d,f,h, where the polar wavetrain is more zonally oriented than the subtropical wavetrain. Hence, despite the high complexity of the atmospheric circulation model used here, the key features (wavenumber and orientation) of the polar wavetrain in Fig.\ \ref{fig:z}d,f,h -- that are associated with the westward migration of the Eurasian ice sheet -- are consistent with linear barotropic theory.

\begin{acknowledgements}
We are grateful to Prof. Johan Kleman for providing the ice-sheet reconstructions. We acknowledge support from the research funding programme "LOEWE-Landesoffensive zur Entwicklung Wissenschaftlich-\"{o}konomischer Exzellenz" of Hesseâs Ministry of Higher Education. The LOEWE initiative also provided financial support for the simulations, which were carried out at the LOEWE Frankfurt Centre for Scientific Computing (LOEWE-CSC). We thank two anonymous reviewers for insightful comments on the manuscript.

\end{acknowledgements}

%% REFERENCES

%% The reference list is compiled as follows:

%\begin{thebibliography}{}

%\bibitem[AUTHOR(YEAR)]{LABEL}
%REFERENCE 1

%\bibitem[AUTHOR(YEAR)]{LABEL}
%REFERENCE 2

%\end{thebibliography}

\bibliographystyle{copernicus}
\bibliography{/home/johan/Latex/references/references.bib}

\clearpage

\begin{figure}[t]
%\includegraphics[width=12cm]{topography~~fig1~~.png}
\caption{Northern Hemisphere topography representative for (a) present-day and PI, (b) MIS5b, (c) MIS4 and (d) LGM, based on the ice-sheet reconstructions in \cite{kleman_etal2013}. The shading represents ice sheets and the contour interval is 500 m.}
\label{fig:kleman}
\end{figure}

\begin{figure}[t]
\includegraphics[width=8cm]{margo_ann.png}
\caption{The colored shading illustrates the simulated annual mean SST anomalies (LGM-PI; in $^\circ$C) in the North Atlantic from the CAM3 simulations using (a) PI OHT and (b) BO2009 OHT \citep{brandefelt+otto2009} as well as (c) the LGM simulation from \cite{brady_etal2013} using the Community Climate System Model version 4 (CCSM4). The equatorward location of the annual-mean sea-ice margin in the respective LGM simulation is depicted by the thick black contours in each panel. The colored markers in each panel show the (annual mean) LGM SST anomaly (LGM-PI) from the MARGO SST reconstruction.}
\label{fig:margo}
\end{figure}

\begin{figure}[t]
%\includegraphics[width=12cm]{~~fig2~~temp.png}
\caption{Boreal summer (JJA) surface temperature (in $^\circ$C) from (a) the ERA-Interim climatology \citep{dee_etal2011}, (b) the present-day simulation, and the EAonly simulations (with PI OHT) of (c) MIS5b, (e) MIS4 and (g) LGM. The position of the zero-degree isotherm is depicted by the green contour. The JJA surface temperature anomalies induced by North American ice sheet (the difference between the fullGlacial and EAonly simulations; in $^\circ$C) are shown in (d,f,h) for (d) MIS5b, (f) MIS4 and (h) LGM. The temperature in the glacial simulations (c to h) has been projected to the present-day orography using the standard lapse rate ($\gamma = -6.5 \times 10^{-3}$ K m^{-1}). The dashed black contours depict the outlines of the \cite{kleman_etal2013} ice-sheet reconstructions in Eurasia and North America. The colored shading in (d,f,h) shows only statistically significant values based on a Student's t-test (at the 95\% confidence level).}
\label{fig:temp}
\end{figure}

\begin{figure}[t]
%\includegraphics[width=12cm]{~~fig3~~precip.png}
\caption{Annual precipitation (in m) from (a) the ERA-Interim climatology \citep{dee_etal2011}, (b) the present-day simulation, and the EAonly simulations (with PI OHT) of (c) MIS5b, (e) MIS4 and (g) LGM. The annual precipitation anomalies induced by North American ice sheet (the difference between the fullGlacial and EAonly simulations; in m) are shown in (d,f,h) for (d) MIS5b, (f) MIS4 and (h) LGM. The dashed black contours depict the outlines of the \cite{kleman_etal2013} ice-sheet reconstructions in Eurasia and North America. The colored shading in (d,f,h) shows only statistically significant values based on a Student's t-test (at the 95\% confidence level).}
\label{fig:precip}
\end{figure}

\begin{figure}[t]
%\includegraphics[width=12cm]{~~fig4~~z300700.png}
\caption{Same as Fig.\ \ref{fig:precip} but for the JJA geopotential height anomalies (in m; zonal mean subtracted) at 700 hPa (shading) and 300 hPa (black contours in d,f,h; contour interval is 30 m, and negative values are dashed). Positive anomalies refer to a anticyclonic circulation anomaly, and negative anomalies to a cyclonic circulation anomaly. The colored shading in (d,f,h) shows only statistically significant values based on a Student's t-test (at the 95\% confidence level).}
\label{fig:z}
\end{figure}

\begin{figure}[t]
%\includegraphics[width=12cm]{~~fig5~~h_standard.png}
\caption{Simulated equilibrium ice thickness in Eurasia (shading; in km) using the PI OHT climate forcing from the EAonly (a,c,e) and fullGlacial (b,d,f) simulations for MIS5b (a,b), MIS4 (c,d) and LGM (e,f). The dashed black contours depict the outlines of the \cite{kleman_etal2013} ice-sheet reconstructions. The land area in the simulations is indicated by the brown color, and the present-day coastline by the thin black contour. The total Eurasian ice-sheet area in each simulation is indicated in the panel titles.}
\label{fig:h}
\end{figure}

\begin{figure}[t]
%\includegraphics[width=8.3cm]{~~fig6~~center_of_mass.png}
\caption{The longitude of the center of mass of ~~the Eurasian ice sheet~~ total ice distribution in Eurasia (λ_c) in the \cite{kleman_etal2013} reconstructions (black bars), EAonly simulations (gray bars), and fullGlacial simulations (white bars).}
\label{fig:center}
\end{figure}

~~\begin{figure}[t]~~
~~%\includegraphics[width=8.3cm]{fig7.png}~~
~~\caption{The stationary wavenumber K_s (Eq.\ \ref{eq:ks}) calculated using the JJA climatology of the zonal-mean zonal wind at 300 hPa from the MIS5b (dashed line), MIS4 (thin solid line) and LGM (thick solid line) EAonly simulations.}~~
~~\label{fig:ks}~~
~~\end{figure}~~

\begin{figure}[t]
%\includegraphics[width=12cm]{~~fig8~~h_q2.png}
\caption{Same as Fig.\ \ref{fig:h} but using the climate forcing from the atmospheric simulations with ~~LGM~~BO2009 OHT.}
\label{fig:h_q2}
\end{figure}

```
\begin{figure}[t]
%\includegraphics[width=12cm]{fig9h_mis5b.png}
\caption{Simulated equilibrium ice thickness in Eurasia (shading; in km) using the MIS5b (with PI
OHT) climate forcing from the EAonly (a,c) and fullGlacial (b,d) simulations. In (a,b), the
simulations were initialized with the reconstructed ice-sheet topography from
\cite{kleman_etal2013}, and in (c,d) the JJA surface temperature was reduced by 3$^\circ$C
throughout the entire simulation.}
\label{fig:h_mis5b}
\end{figure}

\clearpage

\begin{table}[t]
\caption{Top of the atmosphere insolation during the northern summer solstice \citep[60$^\circ$N;]
[]{berger+loutre1991} and greenhouse gas concentrations \citep{petit_etal1999,spahni_etal2005}
in the glacialtime slice simulations.}
\begin{tabular}{lllll}
\tophline
& Insolation & CO$_2$ & CH$_4$ & N$_2$O \\
\middlehline
PI & 475 W m$^{-2}$ & 280 ppm & 760 ppb & 270 ppb \\
MIS5b & 505 W m$^{-2}$ & 210 ppm & 450 ppb & 240 ppb  \\
MIS4 & 490 W m$^{-2}$ & 195 ppm & 460 ppb & 215 ppb  \\
LGM & 480 W m$^{-2}$ & 185 ppm & 350 ppb & 200 ppb \\
\bottomhline
\end{tabular}
\label{table:ghg}
\end{table}

\begin{table}[t]
\caption{Average summer (JJA) temperature in the Northern Hemisphere $\overline{T}_{NH}$, in
Eurasia $\overline{T}_{EA}$ (average within the area 20$^\circ$W, 180$^\circ$E, 45$^\circ$N and
90$^\circ$N), and the average latitude of the zero-degree isotherm $\overline{\phi}_0$ in the PI
OHT simulations.}
\begin{tabular}{llll}
\tophline
 & $\overline{T}_{NH}$ & $\overline{T}_{EA}$ & $\overline{\phi}_0$ \\
\middlehline
Present-day & 21.1$^{\circ}$C & 11.4$^{\circ}$C & 75$^{\circ}$N \\
PI & 18.7$^{\circ}$C & 9.7$^{\circ}$C & 75$^{\circ}$N \\
\middlehline
MIS5b PDoro & 18.3$^{\circ}$C & 9.8$^{\circ}$C & 76$^{\circ}$N  \\
MIS5b EAonly & 18.1$^{\circ}$C & 9.5$^{\circ}$C & 73$^{\circ}$ N \\
MIS5b fullGlacial & 17.5$^{\circ}$C & 9.2$^{\circ}$C & 71$^{\circ}$N  \\
\middlehline
MIS4 PDoro & 17.3$^{\circ}$C & 7.3$^{\circ}$C & 71$^{\circ}$N  \\
MIS4 EAonly & 17.0$^{\circ}$C & 6.2$^{\circ}$C & 67$^{\circ}$N \\
MIS4 fullGlacial & 16.3$^{\circ}$C & 5.3$^{\circ}$C & 64$^{\circ}$N  \\
\middlehline
LGM PDoro & 16.3$^{\circ}$C & 6.6$^{\circ}$C & 70$^{\circ}$N  \\
LGM EAonly & 15.9$^{\circ}$C & 4.5$^{\circ}$C & 66$^{\circ}$N  \\
LGM fullGlacial & 14.0$^{\circ}$C & 3.7$^{\circ}$C & 57$^{\circ}$N  \\
\bottomhline
\end{tabular}
\label{table:temp}
```

```
\end{table}

\end{document}
```